Enhanced Underwater Acoustic Communication via Active Field Control

Chaoxian Qi*, Chenpei Huang*, Neil J. A. Egarguin‡, Daniel Onofrei†, Miao Pan*, Jiefu Chen*

*Department of Electrical and Computer Engineering, University of Houston, Houston, TX 77004 USA

‡Institute of Mathematical Sciences and Physics, University of the Philippines Los Baños, Laguna 4030 Philippines

†Department of Mathematics, University of Houston, Houston, TX 77004 USA

ABSTRACT

In this paper, an active source control scheme for manipulation of the acoustic field in ocean environment is presented. This active field control is formulated as an inverse source problem, where the target is to maximize the radiated power in several far directions while keeping a low radiated power in one or more other far field regions. Hence, the controlled source enables acoustic beamforming, i.e., enhancing the acoustic wave-based underwater wireless communication. Numerical simulations are performed to demonstrate the good performance of the proposed method.

KEYWORDS

Active acoustic field control, underwater wireless communication, shallow-water model, inverse source problem

ACM Reference Format:

Chaoxian Qi*, Chenpei Huang*, Neil J. A. Egarguin‡, Daniel Onofrei†, Miao Pan*, Jiefu Chen*. 2021. Enhanced Underwater Acoustic Communication via Active Field Control. In *The 15th International Conference on Underwater Networks & Systems (WUWNet'21), November 22–24, 2021, Shenzhen, Guangdong, China.* ACM, New York, NY, USA, 2 pages. https://doi.org/10.1145/3491315.3491367

1 INTRODUCTION

Active field control is an emerging area in modern acoustics. The current literature has significantly addressed the idea of the active control of the Helmholtz scalar fields in broad applications, including active noise control, active acoustic cloaking and remote sensing [1, 4]. Active acoustic field control in underwater environments is more spread and necessary, especially in underwater acoustic communications (UWA). We propose to utilize the active field control for UWA, which focuses beams to increase the signal-to-noise ratio (SNR) and keeps null regions to mitigate the interference.

In this paper, we consider multiple hydrophones carried by light-weight and soft robotic fish swarm [2]. The active field control problem is formulated as an inverse source-type problem. Our goal is to characterize the inputs required at the hydrophones so that the radiated fields satisfy a series of constraints. For example, radiated power is maximized in several given directions while it is suppressed in some other prescribed directions. The focused beams

Permission to make digital or hard copies of part or all of this work for personal or classroom use is granted without fee provided that copies are not made or distributed for profit or commercial advantage and that copies bear this notice and the full citation on the first page. Copyrights for third-party components of this work must be honored. For all other uses, contact the owner/author(s).

WUWNet'21, November 22–24, 2021, Shenzhen, Guangdong, China © 2021 Copyright held by the owner/author(s).

© 2021 Copyright held by the owner/at ACM ISBN 978-1-4503-9562-5/21/11.

https://doi.org/10.1145/3491315.3491367



Figure 1: Active source control in ocean environments.

can transmit messages to the underwater sensors or the surface station, as shown in Fig. 1. On the other hand, the power is suppressed in the areas for marine habitat and fauna protection and interference cancellation. We consider a shallow water environment with a constant depth. The controlled source is also able to maintain the power assumption within a realistic budget.

2 METHOD

In this section, the numerical approach is elaborated. We consider the discrete sources that can be realized by robotic fish swarm in practice, as an antenna array. We focus on a shallow water homogeneous ocean model based on the rigorous theoretical analysis. In the shallow water environment, the depth is a constant h, the air-water interface (z = 0) is pressure release boundary, and the sea floor (z = -h) is sound-hard boundary. The sketch of the active field control geometry is shown in Fig. 2, where three prescribed far-field directions are displayed, including C_d , C_N , and C_u . The subscript d, N, and u denote the down-link, null, and up-link, respectively. The acoustic beams are focused on \mathcal{C}_d and \mathcal{C}_u , while the radiated field in C_N is canceled out. The simplified geometry is in cylindrical coordinate, i.e., $R_h^3 = \{(\mathbf{x}, z) | \mathbf{x} = (r, \theta)\}$ with $r \in [0, \infty)$, $\theta \in [0, 2\pi)$, and $z \in [-h, 0]$. Then for a point source located at $(\mathbf{x}', \mathbf{z}') = (r', \theta', \mathbf{z}')$, the Green's function \mathcal{G} satisfied the Helmholtz equation,

$$\begin{cases} \nabla^{2} \mathcal{G} + k^{2} \mathcal{G} = -\delta(z - z') \frac{\delta(|\mathbf{x} - \mathbf{x}'|)}{2\pi |\mathbf{x} - \mathbf{x}'|} \\ \mathcal{G} = 0, \text{ at } z = 0 \\ \frac{\partial \mathcal{G}}{\partial z} = 0, \text{ at } z = -h \end{cases}$$
 (1)

The outgoing waves subject to a radiation condition is calculated by normal mode representation of \mathcal{G} . Through asymptotic analysis for $|\mathbf{x}| \to \infty$ and algebraic manipulations of \mathcal{G} , we can obtain the propagating far field pattern \mathcal{F} at a direction (θ, z) due to the point

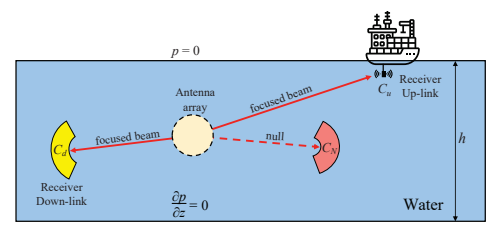


Figure 2: A sketch of the active field control geometry.

source at (r', θ', z') as

$$\mathcal{F}(\theta, z, r', \theta', z') = \sqrt{\frac{2}{\pi}} \sum_{n=0}^{\infty} \sum_{m=0}^{\infty} e^{-i(m + \frac{1}{2})\frac{\pi}{2}} \alpha_{mn}(\theta, z, r', \theta', z'),$$
(2)

where α_{mn} is a Bessel-type function and more details are available in [3, 5]. L point sources (fish swarm in practice) are located at (r'_i, θ'_i, z'_i) , $i = \overline{1, L}$ with amplitudes given by the vector of coefficients $\mathbf{A} = (A_1, ..., A_L)$. The far field pattern generated by these point sources on a far field sector $C = C_d \cup C_u \cup C_N$ can be calculated using the forward operator $\mathcal{K} : \mathbb{C}^L \to L^2(C)$,

$$KA(\theta, z) = \sum_{i=1}^{L} A_i \mathcal{F}(\theta, z, r_i', \theta_i', z_i'), \tag{3}$$

where $\mathbf{A} = (A_1, ..., A_L)$ is the discrete unknown coefficient vector to be characterized. In general, once the forward propagator \mathcal{K} is obtained we can formulate our objective function as,

$$\mathbf{A_{d}} = \underset{\lambda}{\arg\max} \left[\|\mathcal{K}\mathbf{A}\|_{L^{2}(C_{d})}^{2} + \lambda^{2} \|\mathcal{K}\mathbf{A}\|_{L^{2}(C_{u})}^{2} \right],$$
s.t. $\|\mathcal{K}\mathbf{A}\|_{L^{2}(C_{N})}^{2} \approx 0,$ (4)

where the λ is a weighting parameter. A_d is the optimal input amplitudes of the elements in the antenna array.

3 NUMERICAL RESULTS AND DISCUSSION

In this section, simulations are presented to backup the proposed method in Sec. 2. We assume two receivers located in the far field sectors in Fig. 2. The far field sectors are defined as $C_d = \{(\theta, z), \theta \in$ $[179.5^{\circ}, 180.5^{\circ}], z \in [-60, -40]\}, C_u = \{(\theta, z), \theta \in [44.5^{\circ}, 45.5^{\circ}], z \in [44.5^{\circ}, 45.5^{\circ}]\}$ [-12, -10]}, and $C_N = \{(\theta, z), \theta \in [-0.5^\circ, 0.5^\circ], z \in [-52, -48]\}$. In the simulation, the wavenumber k is 40 rad m⁻¹. Two swarms of 20 point sources each (L = 40) are used to achieve the desired effects on the sectors C_d , C_u and C_N defined above. We also assume that the density of water is $\rho = 1020 \, \text{kg/m}^3$ and the sound speed in the water is $c = 1515 \text{ kg m}^{-1}$. We obtain the solution A_d that gives the desired effect in controlled regions. The source power and the pressure due to each source at a point 1 m away is shown in Fig. 3. The reference power level is 1 pW and the reference pressure level is $1 \mu Pa$. The maximum power used on a single source is about 60.89dB while the average power in the swarm is 38.75 dB. The projected power levels on these sectors are shown in Fig. 4. We notice that the swarm of sources projects good power levels at the sectors C_d and C_u and a low amplitude at C_N . These power levels are calculated at each point on the sectors considering the cylindrical spreading associated with the model as $10 \log_{10} \left(\frac{|F|^2}{R\rho c \cdot 10^{-12}} \right)$, where R is the distance between the sources and the receivers, here R = 1000 m. Note that in the receiving area, C_d and C_u , $\|\mathcal{K}A\|_{L^2(C_d)}^2 = 0.0280$

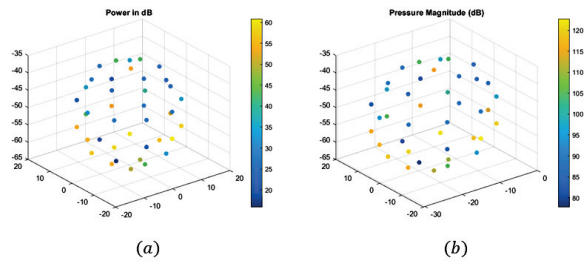


Figure 3: Characterization of the source distribution: (a) Source power. (b) Radiated pressure (1 m away).

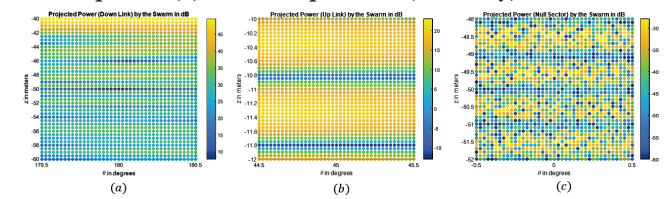


Figure 4: Projected power by the swarm on the sectors: (a) C_d . (b) C_u . (c) C_N .

and $\|\mathcal{K}A\|_{L^2(C_u)}^2 = 1.74 \times 10^{-5}$, which are respectively about 1718 and 529 times what a unit point source will produce. The pointwise projected power ranges between 5 and 50 dB in C_d , -15 and 25 dB in C_u while it is below -27.91 dB all throughout C_N .

4 CONCLUSION

In this paper, the active manipulation of acoustic fields in underwater environment is addressed. We develop a theoretical analysis to characterize acoustic sources with optimal power assumption for desired control effects. The simulation results indicate controlled sources can project significant power level in the desired far-field directions while maintaining null field in some undesired directions.

ACKNOWLEDGMENTS

The work of C. Qi, C. Huang, M. Pan and J. Chen was supported in part by the U.S. National Science Foundation under grant CNS-1801925 and federal funding from the Department of the Treasury through the State of Texas under the Resources and Ecosystems Sustainability, Tourist Opportunities, and Revived Economies of the Gulf Coast States Act of 2012 (RESTORE Act).

REFERENCES

- Jordan Cheer. 2016. Active control of scattered acoustic fields: Cancellation, reproduction and cloaking. The Journal of the Acoustical Society of America 140, 3 (2016), 1502–1512. https://doi.org/10.1121/1.4962284
- [2] Zheng Chen. 2017. A review on robotic fish enabled by ionic polymer-metal composite artificial muscles. *Robotics and biomimetics* 4, 1 (2017), 24. https://doi.org/10.1186/s40638-017-0081-3
- [3] Neil Jerome A Egarguin, Daniel Onofrei, Chaoxian Qi, and Jiefu Chen. 2020. Active manipulation of Helmholtz scalar fields: near-field synthesis with directional farfield control. *Inverse Problems* 36, 9 (2020), 095005. https://doi.org/10.1088/1361-6420/aba106
- [4] Stephen J Elliott, Woomin Jung, and Jordan Cheer. 2019. Causality and robustness in the remote sensing of acoustic pressure, with application to local active sound control. In ICASSP 2019-2019 IEEE International Conference on Acoustics, Speech and Signal Processing (ICASSP). IEEE, Brighton, UK, 8484–8488. https://doi.org/10. 1109/ICASSP.2019.8682474
- [5] Chaoxian Qi, Neil Jerome A Egarguin, Daniel Onofrei, and Jiefu Chen. 2021. Feasibility analysis for active near/far field acoustic pattern synthesis in free space and shallow water environments. Acta Acustica 5 (2021), 39. https://doi.org/10. 1109/ICC42927.2021.9500954